Investigation of silver - glass nanocomposites by positron lifetime spectroscopy

1996 J. Phys.: Condens. Matter 8 5649

(http://iopscience.iop.org/0953-8984/8/30/014)

J. Phys.: Condens. Matter **8** (1996) 5649–5657. Printed in the UK

Investigation of silver–glass nanocomposites by positron lifetime spectroscopy

M Mukherjee†, P M G Nambissan‡ and D Chakravorty†§

† Indian Association for the Cultivation of Science, Jadavpur, Calcutta 700 032, India
‡ Saha Institute of Nuclear Physics, 1/AF Bidhannagar, Calcutta 700 064, India

Received 8 February 1996

Abstract. Nanocrystalline silver particles were grown in a glass medium by ion-exchange and reduction techniques and studied by positron lifetime spectroscopy. The particle sizes varied from 5 to about 25 nm as observed by transmission electron microscopy. The positron lifetime spectra of all the samples could be decomposed into three components having lifetimes of around 160 ps, 400 ps and 1500 ps. The first is ascribed to positron annihilation at the interfaces of the nanocrystalline silver and the glass matrix, and it decreases and stabilizes as the silver grain size increases. The second component is explained as arising from positrons trapped and annihilated at the free-volume defects in the glass matrix. The third component arises because of the annihilation of orthopositronium at large free-volume defects. The effects of temperature on the interfacial defects and the processes leading to the formation of additional positron trapping centres are discussed.

1. Introduction

The remarkable improvement in several useful physical properties of crystalline materials with particles or grains of size about a few tens of nanometres holds great promise for the materials science and technology of the future (Schmitt-Ott *et al* 1980, Birringer *et al* 1984, Gleiter 1989, Schaefer *et al* 1989). The improved characteristics of these nanocrystalline materials are in fact due to the presence of a very large number of grain interfaces. As the majority of the atoms reside on these grain interfaces, some of the properties of these materials appear to be controlled by these atoms (Birringer *et al* 1986).

The most well known method of preparation of nanocrystalline materials is the technique incorporating metal evaporation and condensation in a high-purity noble-gas atmosphere (Schaefer *et al* 1988). After evacuation of the noble gas, the ultrafine powder is compacted in a high vacuum under mechanical pressure to disc-shaped pellets. In the present work, we have used an alternative method of growing nanosized silver particles in a glass medium by ion exchange and a suitable reduction treatment. This method has the advantages that the growth of nanocrystalline grains and their interfaces are natural, and no artificial compaction is required. The grain growth can be efficiently controlled by properly choosing the reduction temperature and time.

It is now generally accepted that the properties of nanocrystalline materials are very sensitive to the defect structures and the dynamical processes associated with them. Rather than the commonly encountered crystalline defects, the grain interfaces are the most important

§ Also affiliated to Jawaharlal Nehru Centre for Advanced Scientific Research, Bangalore 560064, India

0953-8984/96/305649+09$19.50

defect structures to be investigated in order to understand the exotic features of nanocrystalline materials. These grain interfaces are distinctly different from the macroscopic grain boundaries in coarse crystalline solids. Several experimental methods have been applied to the investigation of the properties of nanophase materials with varying degrees of success. Transmission electron microscopy (TEM) provides probably the most direct way of characterizing the nanophase structure. Nanocomposite structures have been used in recent years to study the properties of the nanocrystalline state of matter (Roy and Chakravorty 1990). Estimation of the fractal dimensions and measurements of the electrical resistivity have also been carried out by various groups to delineate the mechanisms leading to the anomalous features exhibited by these materials at low temperatures (Mukherjee *et al* 1993, 1994). One of the highly successful spectroscopic probes for the study of the structural aspects of nanocrystalline materials even at subatomic levels incorporates the measurements of positron lifetimes as functions of certain well chosen controlled experimental parameters (Tong *et al* 1992, Qin *et al* 1994, Kizuka *et al* 1994). We report here the results of our investigation by positron lifetime measurements of silver nanoparticles grown in a glass medium by the reduction of ion-exchanged glass at different temperatures.

2. Experimental details

2.1. Preparation of the samples

The glass with the composition 55 mol% SiO_2–12 mol% ZnO–32.2 mol% Li_2O–0.8 mol% P_2O_5 was prepared by melting the required amounts of reagent-grade chemicals in alumina crucibles in an electrically heated furnace at around 1400 °C. The melt was poured onto a brass plate. Several glass plates were cut and powdered by gentle grinding. The samples were subjected to a lithium $\leftrightarrow$ silver ion exchange by immersing them in a molten bath of silver nitrate at a temperature of 310 °C for a period of 8 h. The samples were then washed in distilled water to remove any adhering traces of silver nitrate and dried. These were subjected to reduction treatment in hydrogen at temperatures ranging from 300 to 800 °C. After the reduction, the samples were quenched to room temperature to ensure a narrow size distribution of the silver metal particles. More details have been presented elsewhere (Chatterjee and Chakravorty 1989).

2.2. Transmission electron microscopy

Transmission electron micrographs were taken using a JEM 200 CX microscope operated at 160 kV at the Regional Sophisticated Instrumentation Centre, Bose Institute, Calcutta.

2.3. Positron lifetime measurements

A weak (about 1.5 μCi) ^{22}NaCl source was deposited on and covered by folding a thin (about 2 mg cm^{-2}) nickel foil. It was kept immersed in the centre of a volume of the powdered specimen in a glass tube. The source was covered by the powdered specimen from all sides at least to a thickness of 5 mm so that all the positrons emitted by the source were captured and annihilated in the specimen itself. The glass tube containing the source–specimen assembly was kept such that the source was in between the two detectors of a slow–fast gamma–gamma coincidence spectrometer. The spectrometer had a prompt time resolution (FWHM) of 260 ps. During the positron lifetime data acquisition, the glass tube was continuously evacuated to remove any possible traces of air, which was otherwise

likely to be trapped in the powdered specimen. With a calibration of 50 ps per channel in the multichannel analyser, a total of more than 1 million counts was accumulated for each lifetime spectrum. The spectra were analysed using the programs RESOLUTION and POSITRONFIT (Kirkegaard *et al* 1981). In the multicomponent analysis performed, variances of fit between 0.96 and 1.14 were obtained.

3. Results and discussion

The positron lifetime spectra of two samples are shown in figure 1. The spectra of all the samples were decomposed into three components, called τ_1, τ_2 and τ_3, respectively, in ascending order of their magnitudes. (To avoid scattering of the analysed results, the value of τ_3 was fixed to 1500 ps, which was the mean of the values obtained in an initial unconstrained analysis.) Their respective intensities I_1, I_2 and I_3 were also obtained from the analysis ($I_1 + I_2 + I_3 = 100\%$). The mean positron lifetime $\tau_m = (\tau_1 I_1 + \tau_2 I_2 + \tau_3 I_3)/(I_1 + I_2 + I_3)$ was calculated from these parameters. These values are shown plotted against the reduction temperatures used for the various samples in figure 2.

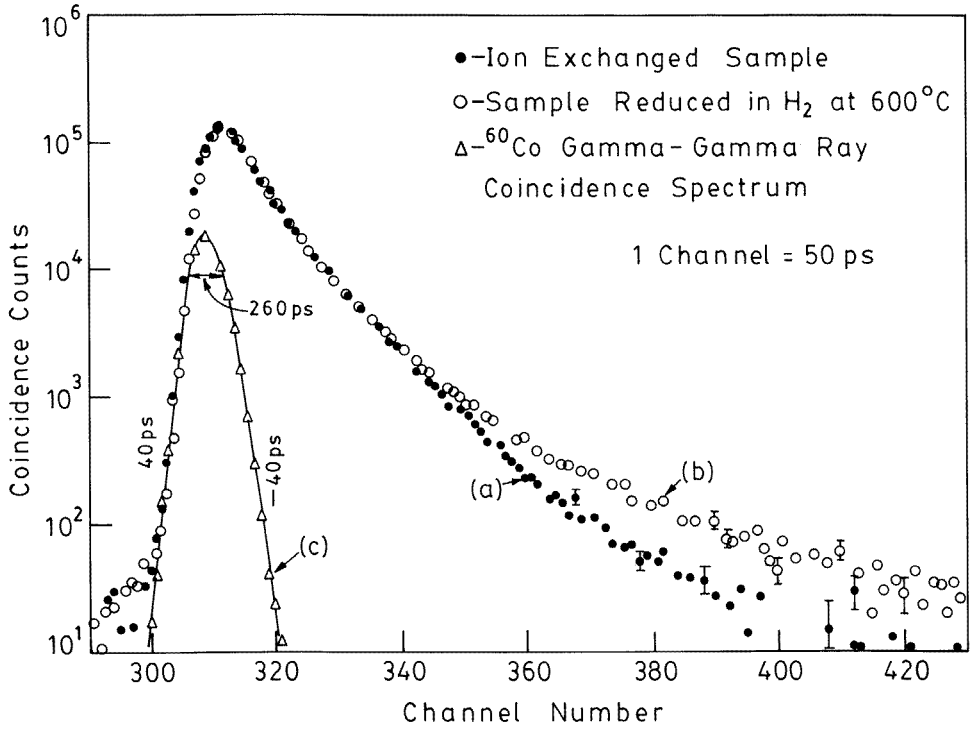

Figure 1. Positron lifetime spectra for (a) the ion-exchanged sample and (b) the sample reduced at 600 °C. (c) The prompt time resolution spectrum of ^{60}Co gamma rays is also shown.

3.1. The origin of the different lifetimes

To understand the physical meaning of the various positron lifetimes, we note that the positrons emitted by the ^{22}Na nuclei became rapidly thermalized on entering the sample. A

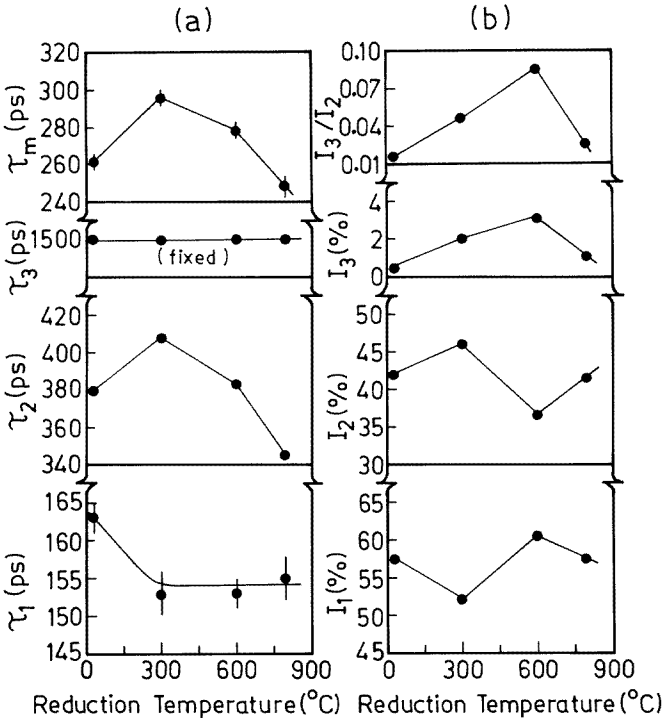

Figure 2. Positron lifetime parameters (a) τ_1, τ_2, τ_3, τ_m and (b) I_1, I_2, I_3, I_3/I_2 plotted as functions of the sample reduction temperature.

significant fraction of these positrons will be captured within the crystalline grains in the sample. If the size of these grains is less than the thermal diffusion wavelength of positrons (about 50–110 nm in most of the materials), they will diffuse out of the grains and become trapped at the grain interfaces. Even the largest grains used in this study have diameters of about 38 nm and are therefore much smaller than the positron thermal diffusion wavelength. Hence all the positrons entering into the grains would eventually diffuse out and annihilate at the grain interfaces. During the analysis of the positron lifetime spectra, specific attempts were made to search for very short-lived components with lifetimes of the order of 50 ps or slightly more (the delocalized positron lifetime of 133 ps shortened by trapping in the grains) but no such lifetimes were obtained. This observation, in other words, ruled out the presence of any kind of positron traps inside the grains. This is further supported by the observations of Matuoka and Morinaga (1982) who reported that there are no positron traps in an ultrafine silver particle of about 70 nm diameter. On the other hand, the disorder in the arrangement of atoms at the grain interfaces, a specific feature of nanocrystalline materials (Schaefer *et al* 1988), can result in 'vacancy-like' trapping centre for positrons. Positrons which are thus trapped and subsequently annihilated at the grain interfaces have been shown to have lifetimes similar to the values of τ_1 obtained in the present work (Qin *et al* 1994, Kizuka *et al* 1994). We therefore attribute the origin of τ_1 in our experiments to positron annihilation at the interfaces of the nanocrystalline silver grains and the glass medium. This argument is further supported by the work by Sui *et al* (1992) who had given similar interpretations in their studies of nanocrystalline Ni–P alloys. Figure 3(a)

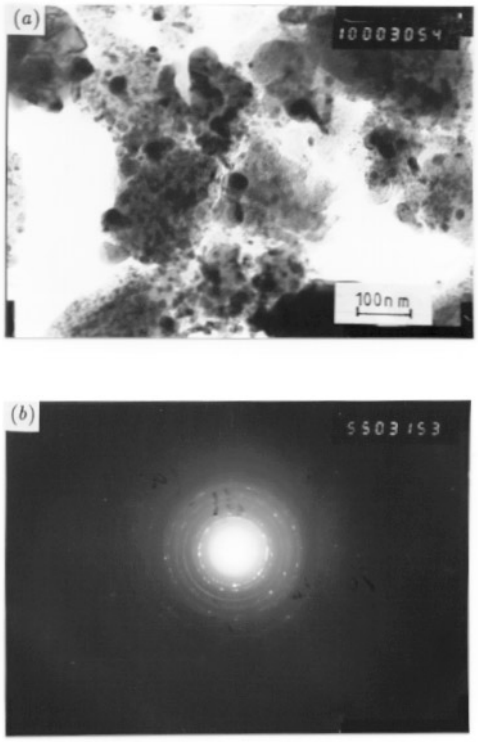

Figure 3. (a) Electron micrograph and (b) the diffractogram of the ion-exchanged sample.

shows the transmission electron micrograph for the ion-exchanged sample. Figure 3(b) is the electron diffraction pattern for figure 3(a). The diffraction rings confirm the presence of metallic silver. In table 1, the experimental and the standard ASTM d_{hkl}-values are listed. The microstructure observed in the case of the ion-exchanged sample is typical of those found for specimens subjected to reduction in hydrogen. The precipitation of colloidal silver within the glass without any hydrogen treatment arises owing to photoreduction of silver ions. It is believed that some impurity ions such as Fe^{2+} present in the glass act as the sensitizer for such a reaction to take place (McMillan 1964). In figure 4 is shown the histogram of silver particles as obtained from figure 3(a). The particle size is found to obey a log-normal distribution function given by

$$\Delta n = (1/\sqrt{2\pi}\ln\sigma)\exp\{-\tfrac{1}{2}[\ln(x/\bar{x})/\ln\sigma]^2\Delta(\ln x) \tag{1}$$

where Δn is the fractional number of particles, x is the diameter of the particles, $\bar{x}$ is the median diameter and σ is the geometric standard deviation. The solid curve in figure 4 is obtained by least-squares fitting of the experimental data to the above equation. Table 2 summarizes the values of $\bar{x}$ and σ obtained for the different samples.

The value of τ_1 obtained in the present work (163 ps) is much higher that that for pure bulk silver (136 ps) (Debowska 1992) but less than that for positrons trapped in monovacancies (186 ps) (Stuck and Schaefer 1985) or in dislocations (200 ps) (Linderoth and Hidalgo 1987) in silver. In the high-pressure compaction studies on nanocrystalline silver, Qin *et al* (1994) had attributed the values of τ_1 ranging from 203 to 164 ps in their work to positron trapping at the vacancy-like defects at the interfaces. The value of 163 ps

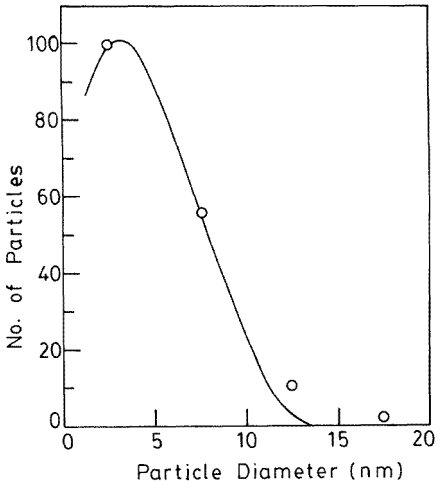

Figure 4. A typical histogram obtained from figure 3(a). The solid curve is the fit obtained using the log-normal distribution.

obtained in the present experiment is more in agreement with the value of 164 ps obtained by Qin *et al* (1994) after the shrinkage of the vacancy-cluster defects and the elimination of vacancy-like defects. Also the fact that the mean size of a defect is less than that of a monovacancy is more characteristic of an interfacial defect rather than a conventional lattice defect (Schaefer *et al* 1988, Kizuka *et al* 1994). In our work, the nanocrystalline grains were formed by the process of nucleation and growth at the reduction temperatures used. This is different from the processes involved in high-pressure compaction.

Table 1. ASTM and observed interplanar spacings d_{hkl} for ion-exchanged sample.

d_{hkl} (nm)		
	ASTM	
Observed	Silver	Silver oxide
0.272		0.2734
0.236	0.2359	0.2365
0.205	0.2044	
0.166		0.1674
0.145	0.1445	0.1427
0.123	0.1231	
0.093	0.09375	

The second lifetime component τ_2 can be identified as originating from positrons trapped and annihilated at the free-volume defects in the glass matrix. These free-volume defects are in fact the counterparts of large three-dimensional cavities called voids in crystalline solids containing defects. Amorphous materials are in general characterized by a free-volume defect density which is a few orders of magnitude higher than that in pure crystalline solids. In the absence of the nanocrystalline silver grains discussed in the previous paragraph, the presence of such a high concentration of free-volume defects would have resulted in the saturation trapping of positrons, that is all the positrons injected into the sample would

Table 2. Reduction treatments, median diameters $\bar{x}$ and geometric standard deviations σ for different samples.

	Reduction treatment			
Sample	Temperature (°C)	Time (min)	$\bar{x}$ (nm)	σ
1	0	0	5.0	1.3
2	300	30	8.7	1.5
3	600	30	10.1	1.6
4	800	30	23.7	1.6

have been trapped and annihilated in these free-volume defects (Mishra *et al* 1981). The magnitude of 380 ps for this lifetime component is typical of positrons trapped in voids of radii 2–3 Å and consisting of the ten to 12 monovacancies per void in crystalline solids (Hautojarvi *et al* 1977). The actual size of the corresponding free-volume defects in the amorphous matrix cannot be very different. The relatively larger value (about 42%) of the intensity I_2 further lends support to the interpretation of positron trapping in free-volume defects.

The long-lived lifetime component $\tau_3 = 1500$ ps (fixed) obtained in the analysis is due to the annihilation of orthopositronium (o-Ps), formed at the internal surfaces of the large free-volume defects. The o-Ps annihilation takes place after the 'pick-off' of the positron from the Ps atom by an electron with opposite spin from the surroundings (Smedskjaer *et al* 1983). The efficiency of this process is dependent on the structure and contamination of the internal surfaces of the defects (Schaefer *et al* 1988). Even in the initial unconstrained positron lifetime data analysis, the values of τ_3 centred around 1500 ps, which was kept fixed in the final analysis. This means that either the large free-volume defects in the glass matrix are contaminated by hydrogen atoms during the reduction treatment or their size is large enough to provide a favourable condition for positronium formation. This interpretation seems to be feasible as the intensity I_3 of this component falls at higher temperatures, as discussed later.

3.2. The results of reduction at higher temperatures

The lifetime τ_1 due to positron annihilation at the grain–glass interfaces falls drastically to 153 ps and remains more or less the same in the samples heat treated at higher temperatures. In agreement with the interpretations given by Tong *et al* (1992), the reduced positron lifetime can be attributed to the shrunken sizes of the positron traps at the interfaces of larger grains. In fact the grain growth would result in the ultimate reduction in the total interfacial area which in turn could lead to shrinkage of the free volume available at the interfaces. It is not known at the present stage what exactly leads to the stabilization of τ_1. Studies over a wider range of grain sizes may throw some light on this problem.

Turning back to figure 2, the variation in τ_1 with the sample reduction temperature is understood in terms of the interpretations given above. However, the variations in the other positron lifetime parameters seem to indicate a number of additional features. The initial rise in τ_2 indicates the agglomeration of the free-volume defects in the glass matrix due to the heat treatment. The sharp decrease in the corresponding intensity I_2 in the temperature range from 300–600 °C provides further support for this argument. The initial rise in I_2 is considered to be the reflection of the decrease in I_1 at this stage due to a

reduction in the total interfacial area brought about by the grain growth. This process in fact continues but its effect on the intensity parameter I_2 becomes less evident because of the dominating effects of the temperature-induced defect agglomeration in the later stages. There is, however, no evidence to suggest whether the largest value of $\tau_2 = 408$ ps observed here is the saturation lifetime in large free-volume agglomerates. The increase in I_3 in the initial stages is accounted for in terms of hydrogen contamination of the internal surfaces of free-volume defect clusters during the reduction at higher temperatures. It may be noted here that an increased 'pick-off' rate had been predicted by Mogensen *et al* (1985) to be due to hydrogen absorption in microcrystals.

The subsequent fall in the value of τ_2, on the other hand, can be understood from the contribution coming from the microvoids formed at the intersection of the interfaces of more than two nanocrystalline grains. During the growth of silver nanoparticles, since the interior of the grain attains crystallinity, the excess free volumes originally present there become transferred out of the grain. These free volumes can then agglomerate at the intersection of the grain interfaces, giving rise to small microvoids. As Schaefer *et al* (1988) had pointed out, the formation of these microvoids is plausible since the atomic positions near the centre of a grain boundary intersection are unstable in the case of strongly differing orientations of the adjoining grains. The positrons trapped in these microvoids may have a characteristic lifetime which is less than the lifetime of positrons annihilating in the free-volume defect agglomerates in the glass matrix. In the case when these two lifetimes are resolution limited, the resultant value of τ_2 will be the weighted average of the two lifetimes. From this viewpoint, the relatively lower values of τ_2 observed in samples containing larger silver grains can be understood in terms of the excess number of microvoids being formed owing to the intersection of nanocrystalline interfaces. This is probable especially when the grains actually grow in size. Also, the rise in the value of I_2 at the final stage further supports this argument. As the positron lifetime at the interfacial intersections cannot be separated from that in the free-volume defects in the glass matrix, the trapping model (Schaefer *et al* 1988) cannot be applied here for the extraction of the residence time of positrons in the delocalized free state.

Do some of the free-volume defect agglomerates in the glass matrix anneal out during the heat treatment? It is reasonable not to rule out the possibility of annealing of at least a fraction of the agglomerates at higher temperatures. I_3 and in fact even the fraction of o-Ps formed in the free-volume defect clusters (indicated by the ratio I_3/I_2 in figure 2) fall significantly beyond 600 °C. The desorption of hydrogen from the defect clusters may begin at this stage, causing the clusters to become unstable and to anneal out. It is reasonable to argue that Ps formation is more favourable in very large vacancy-type defect agglomerates. In smaller vacancy clusters, the overlap between the electron and positron wavefunctions may not be negligible enough to favour the formation of Ps atoms, even though the trapped positron is able to enhance its lifetime. Alternatively, it could be argued that the Ps formation probability is reduced considerably in vacancy clusters of sizes below a certain critical limit. Thus, in the sample which is heat treated at 800 °C, the majority of the vacancy clusters contributing to the value of τ_2 ($= 345$ ps) are microvoids formed at the intersection of the interfaces. A significant fraction of the free-volume agglomerates in the glass matrix may have already been annealed out owing to the relatively higher temperature of the heat treatment.

The behaviour of the mean lifetime τ_m in fact summarizes the above features. Initially the agglomeration of the free-volume defects in the glass matrix results in an increase in τ_m whereas the annealing of these agglomerates and the production of smaller microvoids gradually cause it to decrease at higher reduction temperatures.

4. Conclusions

We have presented here an alternative way of systematically investigating the growth of silver nanoparticles in a glass medium by making use of the ability of positrons to probe sensitively the properties of interfaces of the grains with the glass matrix. The important findings in this study can be summarized as follows.

(i) The lifetime of positrons annihilating at the interfaces of the nanocrystalline grains with the glass reduces and saturates as the average grain size increases. This behaviour is attributed to the shrinkage of the available free volumes at the interfaces during the grain growth.

(ii) In samples heat treated for reduction in hydrogen at higher temperatures, the free-volume defects in the glass matrix agglomerate first but a fraction of them anneal out.

(iii) At higher reduction temperatures, additional trapping centres are generated for positrons at the intersection of nanocrystallite interfaces. These defects are classified as microvoids.

Acknowledgments

The authors thank Professor Prasanta Sen for useful discussions and encouragement. MM and DC acknowledge the support from a foreign research grant N00014-93-1-0040 by Office of Naval Research, Virginia, USA.

References

Birringer R, Gleiter H, Klein H-P and Marquardt P 1984 *Phys. Lett.* **102A** 365
Birringer R, Herr U and Gleiter H 1986 *Trans. Japan Inst. Met. Suppl.* **27** 43
Chatterjee A and Chakravorty D 1989 *J. Phys. D: Appl. Phys.* **22** 1386
Debowska E 1992 *Mater. Sci. Forum* **105–110** 635
Gleiter H 1989 *Prog. Mater. Sci.* **33** 223
Hautojarvi P, Heinio J, Manninen M and Nieminen R 1977 *Phil. Mag.* **35** 973
Kirkegaard P, Eldrup M, Mogensen O E and Pedersen N J 1981 *Comput. Phys. Commun.* **23** 307
Kizuka T, Nakagami Y, Ohata T, Kanazawa I, Ichinose H, Murakami H and Ishida Y 1994 *Phil. Mag.* A **69** 551
Linderoth S and Hidalgo C 1987 *Phys. Rev.* B **36** 4054
Matuoka Y and Morinaga M 1982 *J. Phys. C: Solid State Phys.* **15** 4207
McMillan P W 1964 *Glass Ceramics* (London: Academic)
Mishra T, Otake S, Fukushima H and Doyama M 1981 *J. Phys. F: Met. Phys.* **11** 727 and some of the references therein
Mogensen O E, Eldrup M, Morup S, Ornbo J W and Topsoe H 1985 *Positron Annihilation* ed P C Jain, R M Singru and K P Gopinathan (Singapore: World Scientific) p 980
Mukherjee M, Datta A and Chakravorty D 1994 *Appl. Phys. Lett.* **64** 1159
Mukherjee M, Saha S K and Chakravorty D 1993 *Appl. Phys. Lett.* **63** 42
Qin X Y, Zhu J S, Zhou X Y and Wu X J 1994 *Phys. Lett.* **193A** 335
Roy B and Chakravorty D 1990 *J. Phys.: Condens. Matter* **2** 9323
Schaefer H-E, Eckert W, Stritzke O, Wurschum R and Templ W 1989 *Positron Annihilation* ed L Dorikens-Vanpraet, M Dorikens and D Segers (Singapore: World Scientific) p 79
Schaefer H-E, Wurschum R, Birringer R and Gleiter H 1988 *Phys. Rev.* B **38** 9545
Schmitt-Ott A, Schurtenberger P and Siegman H C 1980 *Phys. Rev. Lett.* **45** 1284
Smedskjaer L C and Fluss M J 1983 *Solid State: Nuclear Methods (Methods of Experimental Physics 21)* ed J N Mundy, S J Rothman, M J Fluss and L C Smedskjaer (New York: Academic) p 78
Stuck W and Schaefer H-E 1985 *Positron Annihilation* ed P C Jain, R M Singru and K P Gopinathan (Singapore: World Scientific) p 454
Sui M L, Xiong L Y, Deng W, Lu K, Patu S and He Y Z 1992 *Mater. Sci. Forum* **105–110** 1249
Tong H Y, Ding B Z, Wang J T, Lu K, Jiang J and Zhu J 1992 *J. Appl. Phys.* **72** 5124